Reconstructing Dark Matter Properties via Gamma-Rays with *Fermi*-LAT

Nicolás BERNAL[*][†]

Bethe Center for Theoretical Physics and Physikalisches Institut, Universität Bonn
Nussallee 12, D-53115 Bonn, Germany
Centro de Física Teórica de Partículas, Instituto Superior Técnico
Avenida Rovisco Pais, 1049-001 Lisboa, Portugal
E-mail: `nicolas@th.physik.uni-bonn.de`

We study the capabilities of the *Fermi*–LAT instrument for identifying particle Dark Matter properties as mass, annihilation cross section and annihilation channels, with gamma-ray observations from the Galactic Center. For the potential Dark Matter signal, besides the prompt gamma-ray flux produced in Dark Matter annihilations, we also take into account the flux produced by inverse Compton scattering of the electrons and positrons generated in Dark Matter annihilations off the interstellar photon background. We show that the addition of this contribution is crucial in the case of annihilations into e^+e^- and $\mu^+\mu^-$ pairs. In addition to the diffuse galactic and extragalactic background, we also consider the full catalog of high-energy gamma-ray point sources detected by *Fermi*. The impact of the degeneracies between the different Dark Matter annihilation channels has been studied. We find that for Dark Matter masses below ~ 200 GeV and for typical thermal annihilation cross sections, it will be possible to obtain stringent bounds on the Dark Matter properties.

---

[*]Speaker.

1. Introduction

If Dark Matter (DM) is detected and identified, the measurement of its properties like mass, annihilation cross-section and annihilation channels plays a central role in the determination of the particle nature of the DM. It will allow us to constrain models of particle physics beyond the Standard Model, for instance supersymmetry and universal extra dimensions. Furthermore a convincing DM discovery may require consistent signals in multiple experiments in multiple channels (direct, indirect, collider). We discuss the capabilities of the *Fermi*–LAT instrument for identifying particle DM properties with gamma-ray observations from the Galactic Center (GC).

The differential intensity of the photon signal from a given observational region in the galactic halo from the annihilation of DM particles has different possible origins: internal bremsstrahlung and secondary photons (prompt) as well as Inverse Compton Scattering (ICS). External bremsstrahlung and synchrotron emission also contribute to the photon flux; however, for the energies of interest here and for typical DM masses, both bremsstrahlung and synchrotron emission are expected to be subdominant with respect to ICS. For the sake of simplicity we will neglect these sources in what follows.

The differential flux of prompt gamma-rays from DM annihilations and coming from a direction within a solid angle $\Delta\Omega$ is given by

$$\left(\frac{d\Phi_\gamma}{dE_\gamma}\right)_{\text{prompt}}(E_\gamma, \Delta\Omega) = \frac{\langle\sigma v\rangle}{2m_\chi^2} \sum_i \frac{dN_\gamma^i}{dE_\gamma}\text{BR}_i \frac{1}{4\pi}\int_{\Delta\Omega} d\Omega \int_{\text{los}} \rho\left(r(s,\Omega)\right)^2 ds, \qquad (1.1)$$

where $\langle\sigma v\rangle$ is the total thermally averaged annihilation cross section, m_χ the mass of the DM particle, BR_i the annihilation fraction into channel i, dN_γ^i/dE_γ the differential gamma-ray yield of standard model particles into photons of energy E_γ, $\rho(r)$ the DM density profile and r the distance from the GC. Here we will focus on the NFW halo profile [1]; the dependence on the DM halo profile has been studied in reference [2].

An abundant population of energetic electrons and positrons produced in DM annihilations either directly or indirectly from the hadronization, fragmentation, and subsequent decay of the SM particles in the final states, gives rise to secondary photons at various wavelengths via ICS off the diffuse radiation fields in the galaxy. We approximate this photon background as a superposition of three black-body spectra consisting of the CMB, the optical starlight and the infrared radiation due to rescattering of starlight by dust [3]. The differential flux of high energy photons produced by the ICS processes is given by [4]

$$\left(\frac{d\Phi_\gamma}{dE_\gamma}\right)_{\text{ICS}}(E_\gamma, \Delta\Omega) = \frac{1}{E_\gamma}\frac{1}{4\pi}\int_{\Delta\Omega} d\Omega \int_{\text{los}} ds \int_{m_e}^{m_\chi} dE\, \mathscr{P}(E_\gamma, E)\frac{dn_e}{dE}(E, r, z), \qquad (1.2)$$

where $\mathscr{P}(E_\gamma, E)$ is the differential power emitted into scattered photons of energy E_γ by an electron with energy E. The minimal and maximal energies of the electrons are determined by the electron mass m_e and the DM particle mass. The quantity dn_e/dE is the electron plus positron spectrum after propagation in the Galaxy, which will differ from the energy spectrum produced at the source. We determine the propagated spectrum by solving the diffusion-loss equation that describes the evolution of the energy distribution for electrons and positrons assuming steady state [5]. Regarding the propagation parameters (like diffusion coefficient, energy losses and thickness of the diffusion

zone), we take their values from the commonly used MED model [5]. Again, the dependence on the propagation model has been studied in reference [2].

There are three main components contributing to the high-energy gamma-ray background: the diffuse galactic emission has been estimated by taking the conventional model of the GALPROP code [6]. On the other hand, another source of background particularly important when looking at the GC is that of resolved point sources. We consider all the point sources detected by the first 11 months of *Fermi*–LAT [7] lying in the region of interest. Finally, for the isotropic extragalactic gamma-ray background we used the recent measurements by the *Fermi*–LAT collaboration [8]. For a $10° \times 10°$ region around the GC, the diffuse galactic emission dominates below ~ 20 GeV. Above that value, the emission coming from point sources is the most important. The isotropic extragalactic gamma-ray background is at the percent level.

The Large Area Telescope (*Fermi*–LAT) is the primary instrument on board of the *Fermi Gamma-ray Space Telescope*. It performs an all-sky survey, covering a large energy range for gamma-rays, with an effective area $\simeq 8000$ cm^2 and a field of view of 2.4 sr. In the following analysis, we consider a 5-year mission run, and an energy range from 1 GeV extending up to 300 GeV. We divide this energy interval into 20 evenly spaced logarithmic bins. In order to maximize the signal-to-noise ratio, it has been pointed out that for a NFW profile the best strategy is to focus on a region around the GC of $\sim 10° \times 10°$ [9]. Hence, this is our choice.

2. Reconstructing Dark Matter properties

Once gamma-rays are identified as having been produced in DM annihilations, the next step concerns the possibilities of constraining DM properties [10]. In figure 1 we depict the *Fermi*–
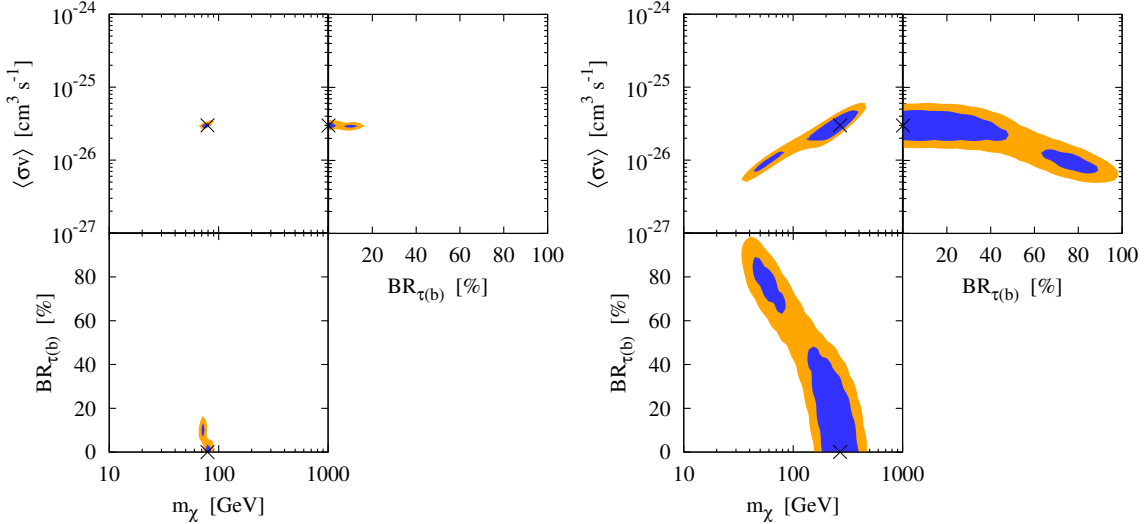
Figure 1: *Fermi*–LAT abilities to constrain DM properties. We consider DM annihilation into a pure $b\bar{b}$ final state and two DM masses: $m_\chi = 80$ GeV (left panels) and $m_\chi = 270$ GeV (right panels). Dark blue (light orange) regions represent 68% CL (90% CL) contours. We assume a $10° \times 10°$ observational region around the GC, a NFW DM halo profile, the MED propagation model and $\langle \sigma v \rangle = 3 \cdot 10^{-26}$ cm^3 s^{-1}. The black crosses indicate the values of the parameters for the simulated observed "data".

LAT reconstruction prospects after 5 years for DM annihilation into a pure $b\bar{b}$ final state reconstructed as either $\tau^+\tau^-$ or $b\bar{b}$ and two possible DM masses: $m_\chi = 80$ GeV (left panels) and $m_\chi = 270$ GeV (right panels). We also assume DM particle with a typical thermal annihilation cross section $\langle\sigma v\rangle = 3 \cdot 10^{-26}$ cm^3 s^{-1}, the MED propagation model, a NFW DM halo profile and a $10° \times 10°$ observational region around the GC. These benchmark points are represented in the figure by black crosses. The dark blue regions and the light orange regions correspond to the 68% CL and 90% CL contours respectively. The different panels show the results for the planes $(m_\chi, \langle\sigma v\rangle)$, $(\mathrm{BR}_{\tau(b)}, \langle\sigma v\rangle)$ and $(m_\chi, \mathrm{BR}_{\tau(b)})$, marginalizing with respect to the other parameter in each case. $\mathrm{BR}_{\tau(b)} = 100\%$ (0%) corresponds to an annihilation into a pure $\tau^+\tau^-$ $(b\bar{b})$ final state. For the first model chosen in figure 1 (left panels), $m_\chi = 80$ GeV and in general for light DM masses, the reconstruction prospects seem to be promising, allowing the determination of the mass, the annihilation cross section and the annihilation channel at the level of $\sim 20\%$ or better. On the other hand, for heavier DM particles, the regions allowed by data grow considerably worsening the abilities of the experiment to reconstruct DM properties. This is shown for the second model in figure 1 (right panels), $m_\chi = 270$ GeV. In this case, *Fermi*–LAT would only be able to constrain the DM mass to be in the range $\sim (30 - 500)$ GeV and determine the annihilation cross section within an order of magnitude. Let us note the appearance of a second spurious minima corresponding to a lighter mass $m_\chi \sim 60$ GeV, an annihilation cross section $\langle\sigma v\rangle \sim 10^{-26}$ cm^3 s^{-1} and annihilating mainly ($\sim 75\%$) on $\tau^+\tau^-$ pairs.
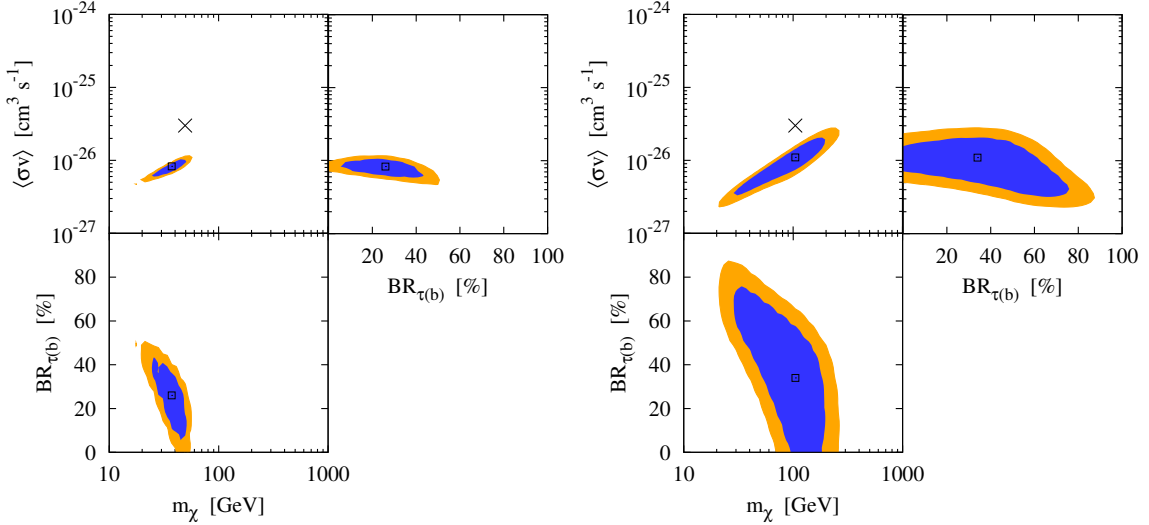
Figure 2: *Fermi*–LAT abilities to constrain DM properties. We assume the measured signal is due to DM annihilating into $\mu^+\mu^-$, but the fit is obtained assuming DM annihilates into either $\tau^+\tau^-$ or $b\bar{b}$. We assume two DM masses: $m_\chi = 50$ GeV (left panels) and $m_\chi = 105$ GeV (right panels). Dark blue (light orange) regions represent the 68% CL (90% CL) contours. See the text for the rest of the parameters. The black cross in the left-top panel in each plot indicates the values of the parameters for the simulated observed "data". Note that the other panels have no cross as they lie outside the parameter space of the simulated observed "data". The squares indicate the best-fit point.

In figure 2 we assume that DM actually annihilates into $\mu^+\mu^-$ pairs, but we analyze the data assuming DM annihilations into either $\tau^+\tau^-$ or $b\bar{b}$, for $\langle\sigma v\rangle = 3 \cdot 10^{-26}$ cm^3 s^{-1} and for two DM

masses: $m_\chi = 50$ GeV (left panels) and $m_\chi = 105$ GeV (right panels). Again, the black crosses indicate the values of the parameters for the simulated observed "data"; the squares indicate the best-fit points. Naïvely, one would expect that the $\mu^+\mu^-$ (leptonic) channel is identified as being closer to the $\tau^+\tau^-$ (leptonic) channel than to the $b\bar{b}$ (hadronic) channel. Let us remember that DM annihilation channels are commonly classified into two broad classes: hadronic and leptonic channels. Leptonic channels typically give rise to a harder spectrum and, in particular for e^+e^- and $\mu^+\mu^-$, the cutoff is be very sharp and around a maximum energy (i.e. the mass of the DM particle in the case on annihilating DM). Contrary to what was expected, the reconstructed composition of the annihilation channels tends to be dominated by $b\bar{b}$, instead of $\tau^+\tau^-$. Indeed, the contribution due to ICS in the case of the $\mu^+\mu^-$ (and also the e^+e^-) channel could substantially alter the different prompt spectra. Hence, when taking into account the contribution of ICS to the gamma-ray spectrum, the annihilation channels cannot be generically classified as hadronic or leptonic, as DM annihilations into $\mu^+\mu^-$ pairs are better reproduced with the $b\bar{b}$ channels than with the $\tau^+\tau^-$ channel.
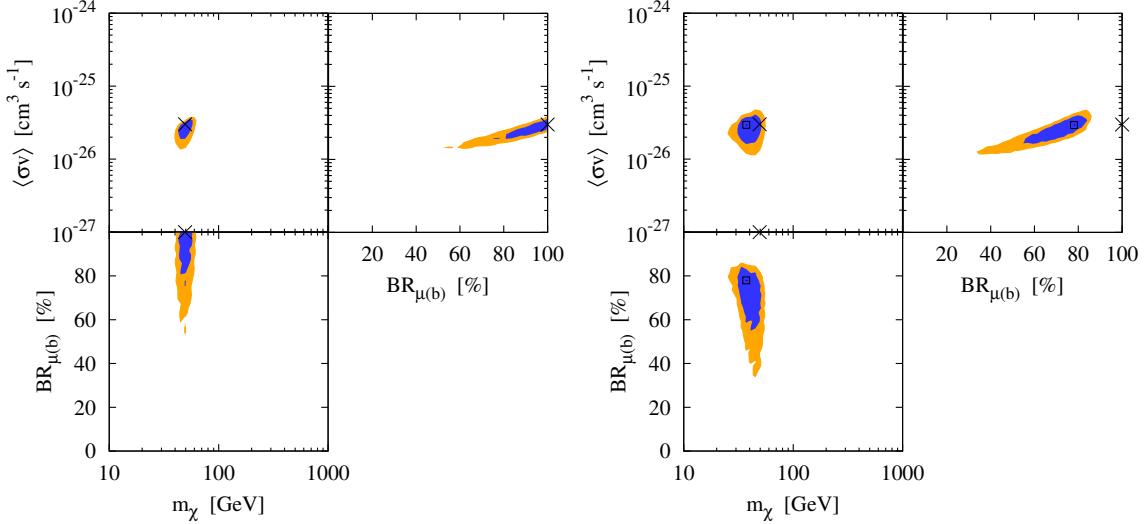
Figure 3: *Fermi*–LAT abilities to constrain DM properties. We assume the measured signal is due to DM annihilating into $\mu^+\mu^-$ and the fit is obtained assuming DM annihilates into $\mu^+\mu^-$ or $b\bar{b}$. We assume ICS+prompt photons (left panels) or only prompt photons (right panels) for the reconstructed signal, for $m_\chi = 50$ GeV. Dark blue (light orange) regions represent the 68% CL (90% CL) contours. See the text for the rest of the parameters. The black crosses indicate the values of the parameters for the simulated observed "data". The squares in the right panels indicate the best-fit point.

The results just discussed can be illustrated in a different way by analyzing the simulated observed signal "data" from DM annihilation into $\mu^+\mu^-$ assuming DM annihilates into either $\mu^+\mu^-$ or $b\bar{b}$. This is depicted in figure 3 where we show the results for the case that we try to reconstruct the full signal (prompt and ICS) generated by a 50 GeV DM particle adding the ICS contribution (left panels) or with only prompt photons (right panels). As can be seen in the left panels, if ICS is taken into account, DM properties can be reconstructed with good precision. However, if the ICS contribution is not added to the simulated signal events (the simulated observed

"data" always has the ICS included), DM annihilation into a pure $\mu^+\mu^-$ channel would be excluded at more 90% CL, providing thus a completely wrong result.

3. Conclusions

In this work we have studied the abilities of the *Fermi*–LAT instrument to constrain Dark Matter properties by using the current and future observations of gamma-rays from the Galactic Center produced by DM annihilations. Unlike previous works, we also take into account the contribution to the gamma-ray spectrum from ICS of electrons and positrons produced in DM annihilations off the ambient photon background. We show that the inclusion of the ICS contribution for hadronic channels and for the $\tau^+\tau^-$ channel does not give rise to important differences in the reconstruction process. This is not the case if DM annihilates into the $\mu^+\mu^-$ and the e^+e^- channel. In this latter case, adding the ICS contribution to the prompt gamma-ray spectrum turns out to be crucial in order not to obtain completely wrong results.

On the other hand, we found that for Dark Matter masses below ~ 200 GeV and for typical thermal annihilation cross sections, it will be possible to obtain stringent bounds on the Dark Matter properties such as its mass, annihilation cross section and annihilation channels.

References

[1] J. F. Navarro, C. S. Frenk and S. D. M. White, Astrophys. J. **462** (1996) 563 [arXiv:astro-ph/9508025].

[2] N. Bernal and S. Palomares-Ruiz, arXiv:1006.0477 [astro-ph.HE].

[3] T. A. Porter and A. W. Strong, arXiv:astro-ph/0507119; T. A. Porter, I. V. Moskalenko, A. W. Strong, E. Orlando and L. Bouchet, Astrophys. J. **682** (2008) 400 [arXiv:0804.1774 [astro-ph]]; M. Cirelli and P. Panci, Nucl. Phys. B **821** (2009) 399 [arXiv:0904.3830 [astro-ph.CO]].

[4] G. R. Blumenthal and R. J. Gould, Rev. Mod. Phys. **42** (1970) 237.

[5] V. L. Ginzburg and S. L. Syrovatskii, New York, Gordon and Breach, 1969; E. A. Baltz and J. Edsjö, Phys. Rev. D **59** (1998) 023511 [arXiv:astro-ph/9808243]; T. Delahaye, R. Lineros, F. Donato, N. Fornengo and P. Salati, Phys. Rev. D **77** (2008) 063527 [arXiv:0712.2312 [astro-ph]].

[6] A. W. Strong and I. V. Moskalenko, Astrophys. J. **509** (1998) 212 [arXiv:astro-ph/9807150]; A. E. Vladimirov *et al.*, arXiv:1008.3642 [astro-ph.HE].

[7] **Fermi-LAT** Collaboration, A. A. Abdo *et al.*, Astrophys. J. Suppl. **188** (2010) 405 [arXiv:1002.2280 [astro-ph.HE]].

[8] **Fermi-LAT** Collaboration, A. A. Abdo *et al.* Phys. Rev. Lett. **104** (2010) 101101 [arXiv:1002.3603 [astro-ph.HE]].

[9] T. E. Jeltema and S. Profumo, JCAP **0811** (2008) 003 [arXiv:0808.2641 [astro-ph]]; P. D. Serpico and G. Zaharijas, Astropart. Phys. **29** (2008) 380 [arXiv:0802.3245 [astro-ph]].

[10] S. Dodelson, D. Hooper and P. D. Serpico, Phys. Rev. D **77** (2008) 063512 [arXiv:0711.4621 [astro-ph]]; N. Bernal, A. Goudelis, Y. Mambrini and C. Muñoz, JCAP **0901** (2009) 046 [arXiv:0804.1976 [hep-ph]]; N. Bernal, arXiv:0805.2241 [hep-ph]; T. E. Jeltema and S. Profumo, JCAP **0811** (2008) 003 [arXiv:0808.2641 [astro-ph]]; S. Palomares-Ruiz and J. M. Siegal-Gaskins, JCAP **1007** (2010) 023 [arXiv:1003.1142 [astro-ph.CO]].